Atmospheric Pollution Research 16 (2025) 102431

Contents lists available at ScienceDirect

Atmospheric Pollution Research

journal homepage: www.elsevier.com/locate/apr

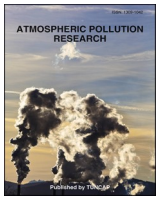

Source apportionment of major ions and trace elements in the atmospheric deposition of Palermo (Sicily, Italy)

Filippo Brugnone [a], Walter D'Alessandro [b], Marcello Liotta [b], Marcello Bitetto [a,b], Luciana Randazzo [a], Sergio Bellomo [b], Lorenzo Brusca [b], Giovanna Cilluffo [a,c], Francesco Parello [a], Sergio Calabrese [a,b,*]

[a] Università degli Studi di Palermo, Dipartimento Scienze della Terra e del Mare, via Archirafi, 36, 90123, Palermo, Italy
[b] Istituto Nazionale di Geofisica e Vulcanologia, Sezione di Palermo, via Ugo la Malfa, 153, 90146, Palermo, Italy
[c] Consorzio Nazionale Interuniversitario per le Scienze del Mare- CONISMA, Roma, Italy

ARTICLE INFO

Keywords:
Atmospheric deposition
Acidity neutralisation
Major ions
Trace elements
Confirmatory factor analysis

ABSTRACT

In Palermo, (Sicily, Italy), a year-long study was conducted to analyse the chemical composition of atmospheric deposition samples. The research was carried out at four urban sites and one semi-rural site. The atmospheric deposition samples were analysed both for major ions and trace elements. Abundances of major ions, on meq L^{-1} basis, followed the sequence $Cl^- > HCO_3^- > NO_3^- > SO_4^{2-} > F^- > Br^-$ for anions, and $Na^+ > Ca^{2+} > NH_4^+ > Mg^{2+} > K^+$ for cations. The statistical technique of Confirmatory Factor Analysis (CFA) was used to identify the main sources of origin of some of the main species and trace elements studied. Ions such as Cl^-, Na^+, Br and I were attributed to the marine source, whilst NH_4^+ and NO_3^- to the anthropogenic source, as well as Mo, Cd, Cu, As, Pb, Sb and V among the trace elements. On the other hand, Ca^{2+}, K^+, Li, Fe, Al, and Sr were mainly of crustal origin. The seawater fractions of Mg^{2+} and SO_4^{2-} were of marine origin, whereas the non-seawater fractions of the same ions were of crustal and anthropogenic origin, respectively. Anthropogenic sources, such as internal-combustion vehicle, domestic heating, and plant emissions, must be considered for Cu, Cr, Ba, Mo, Sb, Zn, As, Ni, and V. This study produced a previously unpublished dataset on the chemical composition of atmospheric deposition that made it possible to identify the main sources influencing air quality in the metropolitan area of Palermo (Italy).

1. Introduction

The chemical composition of atmospheric deposition can be a helpful tool for investigating air pollution levels (Cheng and You, 2010) and estimating the human impact on the atmosphere. However, it is essential to consider that the chemical composition of atmospheric deposition depends on various processes, such as the dissolution of gases and particulate matter emitted by various sources, chemical reactions during local and regional pollutant transport, and removal processes (Arsene et al., 2007; Galy-Lacaux et al., 2009). Atmospheric aerosol particles, including sea salts (usually, the largest fraction of cloud condensation nuclei - CCN), crustal dust, volcanic ash, wildfires, biogenic material, and human-made emissions, are the primary sources of the chemical constituents in atmospheric depositions. Water-soluble and insoluble inorganic components come from both natural and anthropogenic sources. Sodium, chloride, and sea salt sulfate (ss-SO_4^{2-}) are the main components of sea spray (Keene et al., 1986). Calcium and magnesium often originate from soil dust (Safai et al., 2004), and they are usually the main contributors to the neutralisation of rainwater acidity (Prasad Shukla and Mukesh, 2010). On the contrary, non-sea-salt sulfate (nss-SO_4^{2-}) and nitrate are principally derived from the conversion of anthropogenic gaseous precursors, like SO_x and NO_x (Seinfeld and Pandis, 1998). Sulfur dioxide and nss-SO_4^{2-} are emitted by coal-fired power stations, ore smelting, chemical plants, and cruise and cargo ships. Gaseous NO_x is mainly emitted as NO from natural (biogenic emissions and biomass burning during wildfires), and anthropogenic sources (household combustion, fossil fuel combustion in urban transport) (Conradie et al., 2016). It is widely accepted that sulfur and nitrogen components are the primary contributors to the acidification of rainwater (Seinfeld and Pandis, 1998; Huang et al., 2008). When marine air masses cross areas characterised by polluting activities, anthropogenic HNO_3 may react with the marine particles of sodium chloride

* Corresponding author. Università degli Studi di Palermo, Dipartimento Scienze della Terra e del Mare, via Archirafi, 36, 90123, Palermo, Italy.
E-mail address: sergio.calabrese@unipa.it (S. Calabrese).

https://doi.org/10.1016/j.apr.2025.102431
Received 6 September 2024; Received in revised form 20 January 2025; Accepted 21 January 2025
Available online 23 January 2025

(NaCl), with the formation of HCl (Santos et al., 2011). Sulfur dioxide may hydrate and oxidize in the atmosphere and can form various compounds including sulfur trioxide (SO_3) and sulfuric acid (H_2SO_4) as well as sulfate aerosols (Lelieveld, 1993; Seinfeld and Pandis, 1998; Schmidt et al., 2010). Atmospheric NH_4^+ results from gaseous emissions of ammonia (NH_3) and particles containing NH_4^+. Bacterial decomposition of urea in animal excreta (Schlesinger and Hartley, 1992), wildfires, household combustion of wood (Brocard et al., 1998), and production and agricultural use of fertilisers can be considered the main sources of NH_3.

The purpose of this study is to investigate the chemical composition of atmospheric depositions in the urban area of Palermo located in northwest Sicily, Italy. The study will focus on the major ions and trace elements present in the atmospheric depositions and their natural and anthropogenic sources. The use of the Confirmatory factor analysis (CFA) technique allows to identify three main sources, marine spray, atmospheric particles of continental origin and anthropogenic emissions, responsible for the chemical composition of the atmospheric deposition in the study area. Using this statistical technique, it was possible to associate each of these sources with some of the ionic species and trace elements studied. The research will also include a comparison with previous studies conducted in the same area.

2. Sampling site and climatic setting

2.1. Sampling site

The study was carried out for one year, from January 2015 to January 2016, in the metropolitan area of Palermo, a city of 630.167 inhabitants (ISTAT - January 01, 2023), located on the northwest coast of Sicily, in the middle of the Mediterranean Basin (Fig. 1).

The study area belongs to a geologically complex area. The metropolitan area of Palermo is surrounded by mountains, which result from the piling up of deep-water and carbonate platform tectonic units (Imerese and Panormide - Catalano et al., 2013). The Sicilian orogen links the Southern Apennine and the Calabrian Arc to the Tellian and Atlas systems of North Africa. The Sicilian Fold and Thrust Belt is a segment of the Apennine-Tyrrhenian System, which refers both to the

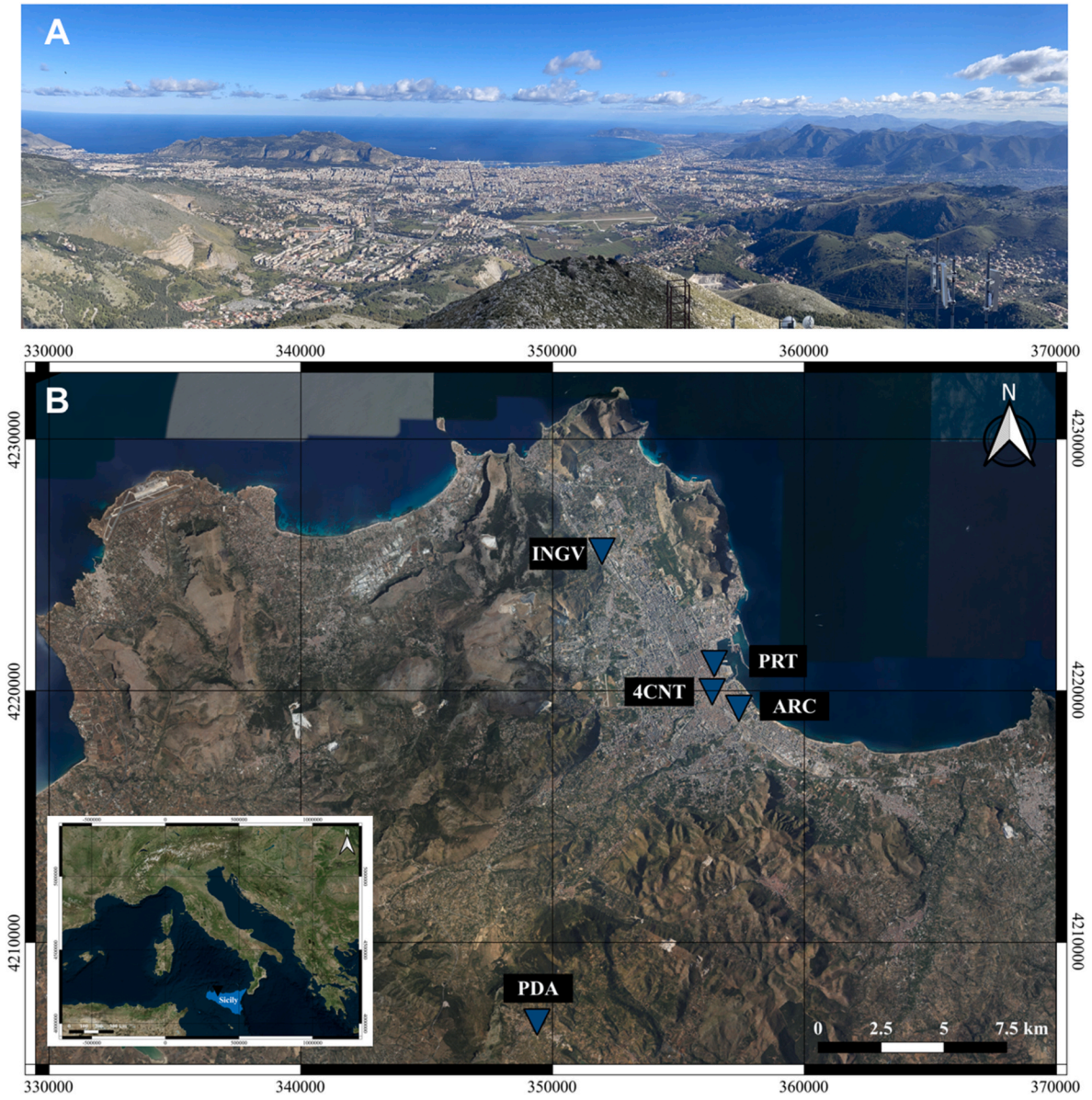

Fig. 1. Localization of the study area (a) and sampling sites (b). Base map Google Earth Pro 7.June 3, 9345. (December 29, 2022). Palermo, Italy. 38° 04′ N, 13° 20′ E, Eye alt 48.8 km. https://www.google.it/earth/download/gep/agree.html (accessed February 26, 2023).

post-collisional convergence between Africa and a complex European crust (Bonardi et al., 2003) and to the coeval roll-back of the subduction hinge of the Adriatic Ionian-African lithosphere (Doglioni et al., 1999; Catalano et al., 2013).

The Palermo urban area is densely populated and serves as a significant cultural and commercial hub in Sicily. The primary contributors to gas and atmospheric particulate emissions are vehicle traffic, domestic heating, and ships, especially cruise ships that frequently crowd the city's main port, particularly in the summer months.

2.2. Climatic setting

The Mediterranean Sea is a significant source of energy and moisture due to evaporation. The evaporation is highest during winter due to the interaction between the sea and the cold and dry air masses coming from the north. The energy and moisture released by the sea are essential elements for cyclogenesis. Due to climate change, cyclogenesis has increased its intensity in recent years, as reported by Mariotti et al. (2002), Lionello et al. (2006), and Gaertner et al. (2007). Knowing the climate setting of the area is crucial to understand the chemical-physical processes that occur in the atmosphere. This helps to recognise the source of atmospheric aerosol particles dispersed by the wind. To obtain an updated assessment of the climatic characteristics of the study area, data from MERRA-2 Modern-Era Retrospective Analysis by NASA (NASA - MERRA-2) were used. The data is relative to the period from January 1970 to December 2020. The Mediterranean region is characterised by a climate of the same name. During February, which is the coldest month of the year, the mean temperatures in the study area range between 9 °C and 14 °C. In contrast, during August, the warmest month of the year, the mean temperatures range between 23 °C and 30 °C. There are peaks even above 45 °C in the presence of adiabatic winds from the south. The rainfall is heaviest from November to February. In contrast, during summers, rainfall is rare. The mean yearly amount of rainfall in the area is about 700 mm. Snowfall is now very rare as compared to the past. The direction and intensity of winds in the investigated area are dependent on the season. During summer, Sicily is characterised by subtropical high-pressure cells that ensure stable weather conditions. The weather conditions are dominated by breezes that blow from the sea to the coast during the day and from the inland to the sea during the night. In winter, cyclonic storms coming from the Atlantic Ocean dominate the weather conditions (Bolle, 2003). The prevailing direction of the winds is about 63% from North and West. The mean wind speed in winter is higher than in summer. The meteorological conditions, i.e., average daily temperature (°C), average daily relative humidity (%), and daily rainfall (L m^{-2}) that characterised the city of Palermo during the study period, i.e. from January 2015 to January 2016, are shown in Fig. S1 (Supplementary Materials). The plotted data were provided by the *Servizio Informativo Agrometeorologico Siciliano - SIAS* of the *Assessorato Risorse Agricole e Alimentari – Dipartimento Interventi Infrastrutturali* of the Sicilian Region and relate to the Palermo weather station (Position UTM WGS84: 353421.3 E, 4221537.7 N).

3. Materials and methods

3.1. Materials

One hundred and fifteen samples of atmospheric deposition were collected in Palermo (Sicily) for almost one year, according to the guidelines published by the main international agency involved in the monitoring of atmospheric precipitation (European Monitoring and Evaluation Programme – EMEP/CCC, 2009; APHA et al., 2005; WMO – World Meteorological Organization, 2018). Samples were collected by using a network of four rain collectors installed in the urban area, while one additional rain collector was installed near Piana Degli Albanesi town (local background), about 15 km from the city of Palermo (Fig. 1 and Table 1). All the collectors were installed on the roof of buildings, at variable heights from the ground.

Each rain collector consisted of a 2 L High-Density-Polyethylene (HDPE) bottle and a Polypropylene (PP) Büchner type funnel (Ø 240 mm). The bottle was inserted in a 1.5 m high Polyvinyl Chloride (PVC) funnel to protect it from direct sunlight (Calabrese et al., 2011). (Fig. 2).

The atmospheric deposition collectors were placed about 2 m above the roofs of public and private buildings and were open during the entire exposure period (about two weeks), collecting both wet and dry depositions.

All plastic ware was washed with ultrapure water of 18 MΩ cm resistance (Milli-Q water-purification system, Millipore) and dried under the hood for 24 h to avoid metal contamination. Afterwards, the collectors were stored in clean plastic bags until their exposure in the field. About every fortnight the collectors were removed and replaced by other clean ones. During some sampling periods, the amount of rainwater exceeded the capacity of the collection bottles (2 L), causing them to overflow with consequent sample loss. 41 rain samples (37% of the total) were collected under these conditions. In such cases, the real rainwater amounts were estimated by using data recorded by weather stations located in the vicinity of the monitoring sites. Sample manipulation and analysis were carried out in a clean room and all the subsamples were stored at 4 °C before analysis.

3.2. Analytical methods

Pre-treatment and chemical analyses of the samples were performed at the laboratories of the *Dipartimento di Scienze della Terra e del Mare*, University of Palermo, and the *Istituto Nazionale di Geofisica e Vulcanologia* (INGV), Section of Palermo.

Electric conductivity (EC) and pH were measured in the laboratory with a Crison Conductimeter and Crison pH meter 52–21 combination electrode, within 48 h of sample collection.

Each collected water sample was divided into three sub-samples for different analyses:

(1) unfiltered sub-sample, for the quantification of the total alkalinity (expressed as HCO_3^-) through an automatic Titrator Compact G20, by using 0.01 N HCl.

Table 1
The collector network and information of monitoring sites.

Locality	ID	Type of site	Position UTM WGS84	Altitude (m a.s.l.)	Height from the ground (m)	Distance from the sea (km)
Palermo – Via Archirafi	ARC	Urban	357403.3 E 4219295.0 N	33	13	0.51
Palermo – Quattro Canti	4CNT	Urban	356361.9 E 4219832.8 N	39	12	0.64
Palermo – Porto	PRT	Urban	356384.8 E 4221121.2 N	35	18	1.20
Palermo – CNR-INGV	INGV	Urban	351947.9 E 4225519.4 N	91	15	4.22
Piana degli Albanesi	PDA	Semi-urban	349791.0 E 4207292.0 N	641	12	15.6

Fig. 2. Photos of the rain gauges installed in the different sampling sites.

(2) filtered (with 0.45 μm filter) sub-sample analysed for major anions (NO_3^-, SO_4^{2-}, Cl^- and F^-) through an ion chromatography system (ICS-1100 Dionex) in suppressed mode and equipped with an anion column (AS14A), a pre-column (AG14A) and carbonate-bicarbonate eluent.
(3) filtered (0.45 μm) and acidified (with Ultrapure HNO_3) sub-sample analysed for major cations (Ca^{2+}, K^+, Mg^{2+}, Na^+, NH_4^+) through an ion chromatography system (ICS-1100 Dionex) in suppressed mode and equipped with a cation column (CS12A) and pre-column (CG12A) that works under a continuous flow of methanesulfonic acid with eluent regeneration. The same sub-sample was also analysed for twenty-eight trace elements (Al, As, B, Ba, Be, Br, Ce, Cd, Co, Cr, Cs, Cu, Fe, I, La, Li, Mn, Mo, Ni, Pb, Rb, Sb, Se, Sn, Sr, Ti, Tl, U, V, and Zn) by inductively coupled plasma optical emission and mass spectrometry (ICP-OES, Jobin Yvon Ultima2, and ICP-MS, Agilent 7500-ce).

During dry periods (no rain in the collectors), dry deposition was recovered following the method described by Menichini, 2006): 300 mL of ultrapure water was used to wash both the funnel and the sampling bottle, and the obtained solution/suspension of the dry deposition was treated as described above.

3.3. Quality control and quality assurance

External calibrations were performed with standard solutions obtained by mixing and diluting multi and single-element work solutions (100 mg L^{-1} and 1000 mg L^{-1}, CertiPUR ICP Standards Merck). The calibration routine was done on selected isotopes for each element with 11 calibration points prepared daily in 10 mL polyethene tubes by dilution with 2% nitric acid solution. Element concentrations in the analysed samples were calculated using the software ICP Mass Hunter (version B.01.01). The sensitivity variations were monitored by ^{103}Rh, ^{115}In, and ^{185}Re with 10 μg L^{-1} concentration as an internal standard added directly online. The reproducibility of the chemical analysis was verified by 5 replications for each sample and standard and the RSD was always below 20%. The analytical accuracy of trace element determinations was checked by the analysis of four Certified Reference Materials (TM Rain 04, SLR4, SLRS5, SPSSW1), specific for the analysis of trace elements in fresh and rainwater and the estimated error was between 10 and 15% for Al, Ti, V, Cr, Fe, Co, Cu, Zn, Se and Pb, with all other elements having an error of less than 10%. To evaluate the overall quality of analytical methods and treatment procedures, the charge balance of the cations and anions was calculated. According to the electro-neutrality principle, the sum of positive and negative charges within the water sample should be zero. The acceptable range of ion difference in atmospheric deposition samples is 10% or ±0.2 meq L^{-1} (Alastuey et al., 1999; APHA, AWWA, WEF, 2005). The range ±0.2 meq

L^{-1} can be used for dilute waters having an anion sum <3.0 meq L^{-1}, as the case of the rainwater samples of this research.

The charge balance error of each sample was calculated according to the equation:

$$Charge\ balance = \left(\frac{\sum anions}{\sum cations} - 1\right) x\ 100. \quad (1)$$

Among cations the hydronium ion (H^+) calculated from the initially measured pH values was also considered. The resulting charge balance was between 0.02% and 70%, with an average value of 15%. In 46.5% of the cases (53/114 samples) the calculated error was between 0% to ± 10%, while in 74.6% of the cases (85/114 samples) the calculated error was between 0% to ± 20%. Even though most of the analysed samples fall within the acceptable range for dilute waters (APHA, AWWA, WEF, 2005) a lot of samples displayed cation excess (Fig. S2 - Supplementary Materials). The sometimes-strong deficiency in anions might be attributed to anionic species, such as CH_3COO^-, $HCOO^-$, $C_2O_4^{2-}$, and PO_4^{3-}, which were not investigated in this study.

To ensure the quality of the sampling and analytical procedures, four blank solutions were prepared and analysed. This step is crucial because any chemical reagent or material that interacts with a sample can alter the concentrations of elements present. The method blank involved pouring 300 mL of ultra-pure water into a pre-cleaned bulk collector. Then, 50 mL of this solution was filtered through a 0.45 μm membrane and acidified in a pre-cleaned centrifuge tube using 200 μL of 65% w/v HNO_3 (Merck Suprapur). Most trace elements were below the detection limit; only a few elements (e.g. Al, Zn, Sr, Ba) had concentrations higher than the detection limit, and they were already subtracted from the measured concentrations in the samples (Table S1).

3.4. Statistical methods

Confirmatory Factor Analysis (CFA) is a statistical technique used in many fields to test the hypothesis that the observed variables (indicators) reflect a smaller number of underlying latent constructs (factors). Latent factors, by their nature, are not measured directly. Instead, the observed variables serve as indicators of the latent construct. In other words, CFA is a multivariate statistical technique, and its purpose is to estimate the structure of a set of data by checking how well the measured variables represent the number of latent constructs. CFA results are usually presented in a path diagram consisting of squares and circles for the variables, connected by arrows. The squares represent observed variables or indicators, and the circles represent latent constructs or factors. The arrows from the factor to the observed variables are 'factor loadings'. When standardised, factor loadings can be interpreted as correlations. CFA was carried out to test a model with three factors: crustal, marine, and anthropogenic sources. In our hypothesis Na^+, Cl^-, Br, I, SO_4^{2-} and Mg^{2+} reflect the underlying marine construct; Ca^{2+}, Mg^{2+}, K^+, Sr, Al, Fe, and Li reflect the latent crustal construct; NO_3^-, NH_4^+, SO_4^{2-}, V, Sb, Pb, As, Cu, Cd and Mo are hypothesised to be associated with the anthropogenic factor. Fit indices represent how plausible the estimated model is. Model fit was assessed using the comparative fit index (CFI) (Bentler, 1990), and root mean square error of approximation (RMSEA) (Steiger, 2010). For CFI, values above 0.90 are considered an acceptable fit and above 0.95 a good fit. An RMSEA below 0.10 is considered an acceptable fit and below 0.05 is a good fit.

4. Results

The results of the analysis for all the samples collected, including chemical-physical parameters, concentrations of major ions and trace elements, can be found in Table S1 of the Supplementary Materials. The main statistical parameters for major ions (meq L^{-1}) and trace elements (μg L^{-1}) are presented in Tables 2 and 3, respectively. A total of 110 bulk atmospheric deposition samples were collected. An additional five samples were taken during a dry period from April 17, 2015 to April 29, 2015.

Table 2
Main statistical values of the chemical-physical parameters and major ions (meq L^{-1}).

	Min.	1st quartile	Median	Mean	3rd quartile	Max.
pH	5.23	6.35	6.65	6.81	7.03	9.45
Electric conductivity (μS cm^{-1})	10.9	26.9	45.7	67.2	69.4	446
Major ions (meq L^{-1})						
Cl^-	0.021	0.082	0.196	0.286	0.412	1.395
HCO_3^-	0.022	0.066	0.111	0.193	0.214	1.905
NO_3^-	<LOQ	0.021	0.032	0.068	0.058	0.503
SO_4^{2-}	0.012	0.041	0.051	0.087	0.079	1.273
F^-	<LOQ	0.001	0.002	0.004	0.004	0.028
NH_4^+	<LOQ	0.025	0.074	0.103	0.139	0.747
Ca^{2+}	0.016	0.074	0.130	0.237	0.247	2.154
Mg^{2+}	0.011	0.041	0.064	0.084	0.104	0.346
K^+	0.002	0.005	0.009	0.021	0.012	0.248
Na^+	0.021	0.072	0.177	0.250	0.347	1.271

Table 3
Main statistical values of trace elements concentrations (μg L^{-1}).

Trace elements (μg L^{-1})	Min.	1st quartile	Median	Mean	3rd quartile	Max.
Li	0.010	0.096	0.151	0.204	0.249	1.757
Be	<LOQ	0.004	0.006	0.006	0.008	0.010
B	<LOQ	2.818	3.995	5.115	6.321	33.42
Al	0.353	3.932	8.622	21.51	23.85	200.0
Ti	<LOQ	0.094	0.200	0.497	0.407	7.499
V	0.142	0.313	0.503	1.618	1.034	43.12
Cr	0.011	0.036	0.063	0.106	0.114	1.300
Mn	0.017	0.705	1.275	4.492	1.996	112.5
Fe	0.215	0.948	1.774	4.906	3.534	48.10
Co	<LOQ	0.018	0.028	0.078	0.044	2.030
Ni	<LOQ	0.254	0.417	0.948	0.910	12.39
Cu	0.090	1.135	2.657	16.42	6.420	1154
Zn	1.146	6.457	12.048	21.74	24.53	188.8
As	<LOQ	0.039	0.068	0.197	0.117	3.957
Se	<LOQ	0.060	0.090	0.122	0.125	1.348
Rb	0.060	0.137	0.219	0.537	0.419	9.409
Sr	2.130	5.934	8.048	14.33	13.97	107.5
Mo	<LOQ	0.042	0.059	0.126	0.099	1.311
Cd	<LOQ	0.014	0.019	0.032	0.031	0.254
Sn	<LOQ	0.020	0.025	0.278	0.073	1.940
Sb	0.026	0.059	0.097	0.147	0.160	1.133
Cs	<LOQ	0.002	0.004	0.006	0.007	0.073
Ba	0.696	2.384	3.855	5.983	7.211	33.65
La	0.001	0.004	0.006	0.014	0.011	0.235
Ce	0.001	0.008	0.015	0.029	0.023	0.482
Tl	<LOQ	0.004	0.007	0.009	0.011	0.035
Pb	<LOQ	0.036	0.094	0.330	0.362	5.678
U	<LOQ	0.002	0.003	0.006	0.005	0.070

The pH values ranged between 5.2 and 9.4 with a median value of 6.5, showing a high variability (Fig. 3a). The Electric Conductivity values ranged from 11 μS cm^{-1} to 446 μS cm^{-1} (from 1.0 to 2.8 on a logarithmic basis), with a median value of 46 μS cm^{-1} (1.7, on a Log_{10} basis) (Fig. 3b).

The concentrations of the major ions (on a meq L^{-1} basis) showed the following order of abundance: $Cl^- > HCO_3^- > SO_4^{2-} > NO_3^- > F^-$ > for anions (Fig. S3a – Supplementary Materials), $Na^+ > Ca^{2+} > NH_4^+ > Mg^{2+} > K^+$ for cations (Fig. S3b – Supplementary Materials). The anion abundances were 50.0% for Cl^-, 28.3% for HCO_3^-, 13.0% for SO_4^{2-}, 8.10% for NO_3^-, and 0.5% for F^-. The cationic abundances were 39.0% for Na^+, 28.7% for Ca^{2+}, 16.2% for NH_4^+, 14.1% for Mg^{2+}, and 2.0% for K^+.

Fig. 4a and b shows the concentrations of major ions (meq L^{-1}) and trace elements (μg L^{-1}). Beryllium concentrations are not plotted

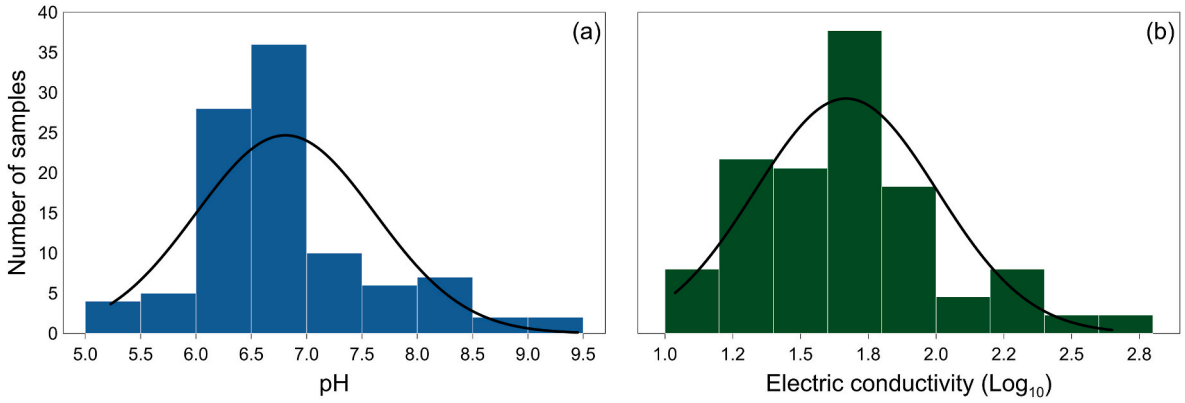

Fig. 3. Frequency distributions of pH (a) and electric conductivity (b) (μS cm^{-1}) values of atmospheric deposition samples.

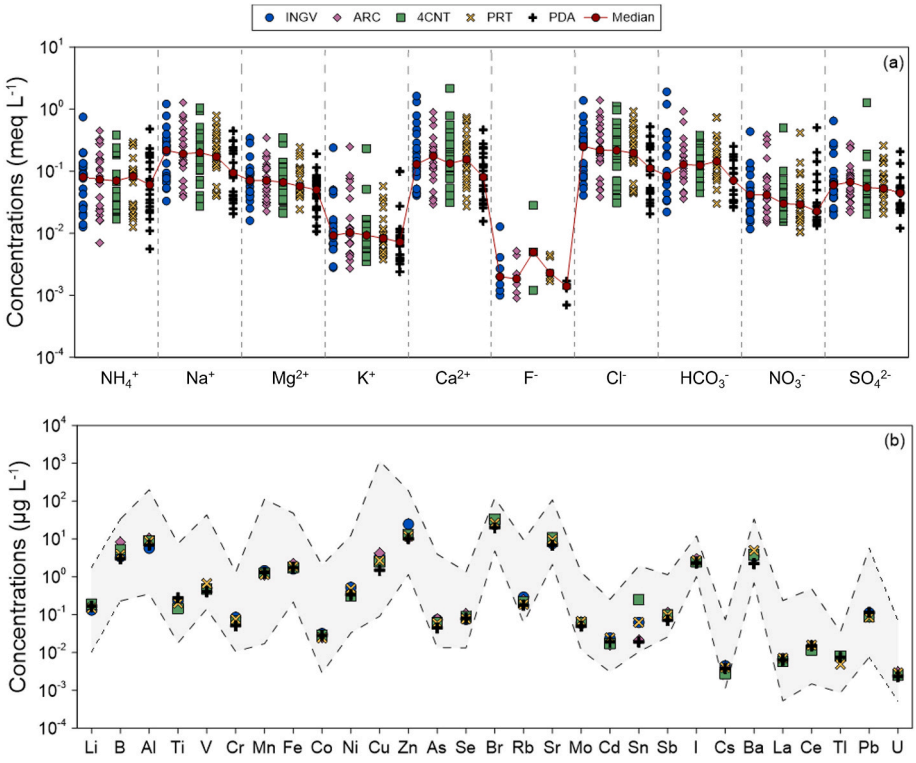

Fig. 4. (a) Concentrations of major elements (meq L^{-1}). Red points, connected by the dotted red line, are the median values for each species and each sampling site. (b) Median concentrations (μg L^{-1}) for trace elements in all the sampling sites; the shaded band encloses the extremes of concentrations (min-max) for each element.

because they were below the quantification limit (LOQ) for most of the samples. While some ions, such as Mg^{2+} and K^{+}, had similar median concentrations across all sampling sites, others like F^{-}, Na^{+}, Cl^{-}, Ca^{2+}, and Zn and Sn (for trace elements) had significant variability, often exceeding one order of magnitude.

By comparing all sites together, using a one-way ANOVA test, we observed no significant differences in the concentrations of the major species (p-value >0.05). Going into more detail, comparing the different monitoring sites in pairs, then some significant differences can be observed (p-value ≤0.05). No significant differences were observed for F^{-}, NO_3^{-}, SO_4^{2-}, K^{+}, and NH_4^{+}. However, significant differences were noted for Cl^{-} and Na^{+} between the ARC site and the PDA site, as well as between the 4CNT site and the PDA site. For Br^{-}, significant differences were only found between the ARC site and the PDA site. In the case of Mg^{2+}, significant differences were observed between the ARC site and the PDA site, as well as between the PRT site and the PDA site. Finally, significant differences in Ca^{2+} were observed between the INGV site and the PDA site and between the PRT site and the PDA site.

For each ionic species and trace element, Fig. S4 (Supplementary Materials) displays the percentage of samples in which the concentration was below the limit of quantification (LOQ).

5. Discussion

Rainwater plays a vital role in cleaning the atmosphere by removing particles and dissolved gaseous pollutants through two scavenging mechanisms: rainout and washout (Kajino and Aikawa, 2015). *Rainout* is the in-cloud scavenging process, which mainly absorbs or condenses gases and fine particles on cloud droplets. *Washout* is the below-cloud scavenging process that efficiently removes coarse particles. The scavenging process in the cloud is related to the activation of cloud condensation nuclei (CCN). These nuclei play a fundamental role in the condensation of water droplets on aerosol particles (Houze, 1993; Liotta et al., 2017). The washout process occurs during the fall of raindrops

from the base of the clouds to the ground. This process can change the chemical composition of the rainwater due to the interaction between the raindrops and the suspended atmospheric particles.

Rainwater is essential for providing nutrients to terrestrial and aquatic ecosystems (Arsene et al., 2007). However, its chemical composition can also cause environmental issues, including acid rain, aquatic eutrophication, and disturbances of biogeochemical cycling (WMO). By studying chemical constituents in rainwater, we can identify the origin, characteristics, concentration, and processes for removing atmospheric pollutants. Long-term variations in the chemical characteristics of atmospheric depositions provide an important tool for evaluating the temporal evolution of atmospheric pollution and can be used as an indicator to evaluate natural processes versus anthropogenic influences (Tang et al., 2005).

5.1. Total dissolved solids (TDS) in atmospheric deposition

In this research, most of the analysed rainwater samples had low Electric Conductivity (EC) values and low amounts of total dissolved solids (TDS), as expected for this natural matrix. However, the EC values showed a wide range of variability, ranging from 10.9 to 446 μS cm^{-1}. The median value of EC for the sampling sites located close to the coastline at distances between 0.4 km and 4.2 km, and in densely urbanised areas was 45.7 μS cm^{-1}. The Piana degli Albanesi sampling site had lower EC values, ranging from 14.3 to 85.0 μS cm^{-1}, with a median value of 31.0 μS cm^{-1}. The EC values were directly proportional to the concentration of ionic species present in the solution (Total Dissolved Solids - TDS) (r = 0.87, p-value <0.0001) (Fig. S5a – Supplementary Materials). The TDS values in the samples of the city of Palermo were higher than those of Piana degli Albanesi, with values ranging from 6.0 mg L^{-1} to 272 mg L^{-1}. This difference was due to a greater contribution, in terms of atmospheric particulates and gaseous species, by marine and anthropogenic (urban) sources in the former area than in the latter. The TDS values were generally inversely correlated with the amount of rain collected, although the correlations were not strong (r = 0.24, p-value = 0.012) (Fig. S5b – Supplementary Materials). As one would expect, the elements that contribute most to the amount of dissolved solids are the major ions, i.e., Na^+, Cl^-, NH_4^+, Ca^{2+}, NO_3^-, SO_4^{2-}, Mg^{2+}, HCO_3^-, K^+, and F^-. In this research, the trace elements making the largest contribution to the TDS of atmospheric deposition samples include, in order, B, Br, Zn, Al, Sr, Fe, Mn, and Ba.

5.2. Major ions and trace elements source apportionment

The concentrations of major ions such as Cl^-, Br^-, SO_4^{2-}, Na^+, K^+, and Mg^{2+} show a variability of two orders of magnitude, while only Ca^{2+} spans three orders of magnitude. The known sources of Na^+ and Cl^- in the urban atmosphere are sea salt (Thurston and Spengler, 1985), crustal aerosols, and incineration operations (only for Cl^-) (Ondov et al., 1982; Kitto, 1993, Wang et al., 2008). Sodium is typically used as a reference to determine the sea-salt component in aerosol particles since the water-soluble Na^+ is assumed to originate solely from seawater. The marine aerosol has a Cl^- to Na^+ molar ratio of 1.16 (Chesselet et al., 1972). Considering this, the high load of Na^+ (from 0.021 to 1.271 meq L^{-1}) and Cl^- (from 0.021 to 1.395 meq L^{-1}) at all sites of the present study were due to the proximity of the study areas to the coast. These two ions had a highly positive correlation (r = 0.99, p < 0.0001) along with a Cl^-/Na^+ ratio corresponding to that of seawater (Fig. 5). This indicates that sea-derived CCN strongly contributed to the chemical composition of the rainwater, while human activities and geogenic dust had a negligible influence on these two ions.

Fig. 5 illustrates the ratio between Na^+ and some ions in the atmospheric deposition samples. Among the ions analysed, Br^- and Mg^{2+} showed a strong correlation with Na^+ (r = 0.89 and r = 0.93 respectively, with p-value <0.0001). However, there was no correlation between Na^+ and other ions such as Ca^{2+}, F^-, NO_3^-, K^+, and SO_4^{2-}. Fig. 6

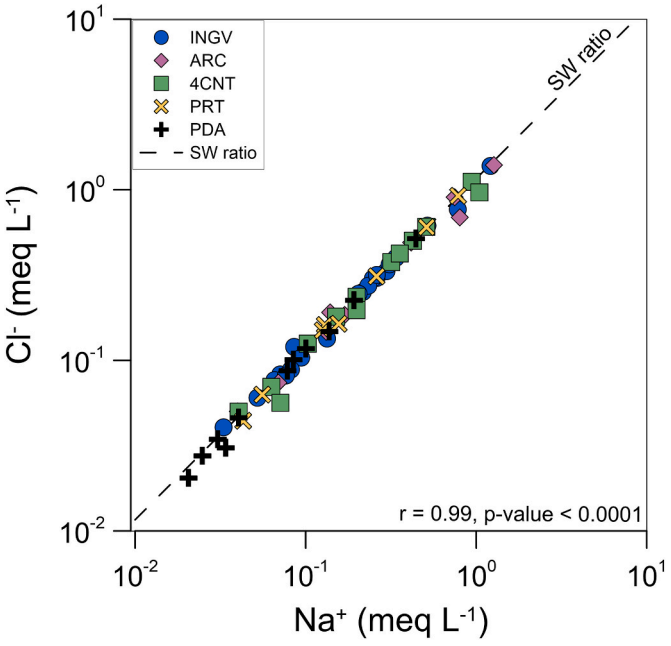

Fig. 5. Correlation between Cl^- and Na^+ (meq L^{-1}) in atmospheric deposition samples.

presents the coefficients of correlation, along with their statistical significance coefficient (p-value) between Na^+ and the other ions. All the major ions were found to be enriched relative to the marine contribution calculated from the ion/Na^+ ratio. The only ion that had a ratio to sodium similar to that of seawater (558) was bromide. With regard to the Mg^{2+}/Na^+ ratio, it was observed that it deviates from that typical of seawater at low Na^+ concentrations, up to about 0.5 meq L^{-1}, highlighting an enrichment of Mg^{2+} correlated with the contribution derived from the crustal source; by increasing the Na^+ concentration, and thus the contribution from the marine source, the ratio of these two ions becomes very close to that typical of seawater (4.47), highlighting a common source between the two species.

The relative contribution of seawater to the total ion composition of the atmospheric deposition was estimated by the equation:

$$[X]marine = [Na^+]rain\ x \left[\frac{X}{Na^+}\right] SW, \quad (2)$$

where $[X]_{marine}$ is the sea salt contribution of X in meq L^{-1}, $[Na^+]_{rain}$ is the concentration of Na^+ in rain (meq L^{-1}), and $[X/Na^+]_{SW}$ is the seawater equivalent ratio (Keene et al., 1986; Conradie et al., 2016).

The non-sea salt fraction of any ion species was calculated by:

$$[X]nss = [X]rain - Na^+_{rain}\ x \left[\frac{X}{Na^+}\right] SW, \quad (3)$$

where [X]rain is the concentration of species X in rainwater, and [X]nss is the non-sea salt contribution of species X in meq L^{-1} (Conradie et al., 2016).

For Na^+ (100%), Cl^- (98.9%), Br^- (90.7%), and Mg^{2+} (68.2%) the predominant source was marine, for NH_4^+ (100%), NO_3^- (100%), F^- (98.4%), Ca^{2+} (93.7%), SO_4^{2-} (61.9%), and K^+ (58.7%) the prevalent source was non-marine (Fig. 7).

The monitoring sites INGV and ARC recorded the highest concentration of Na^+ and ss-Cl^-, with median concentrations of 0.22 and 0.20 meq L^{-1} for the former, and 0.25 and 0.22 meq L^{-1} for the latter, respectively. The median concentration of Na^+ and ss-Cl^- at the monitoring sites in Palermo city was higher than that recorded for the Piana degli Albanesi site (0.19 vs. 0.09 meq L^{-1} for Na^+, 0.23 vs. 0.11 meq L^{-1} for ss-Cl^-). These results indicate that the marine source has a decreasing

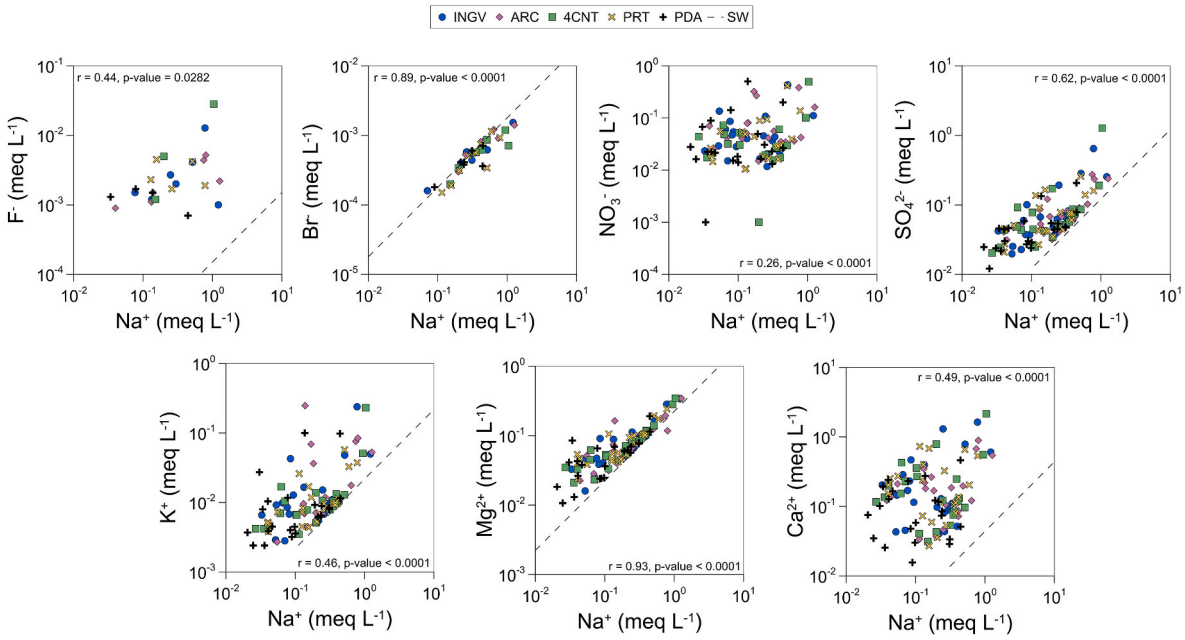

Fig. 6. Na^{+} versus F^{-}, Br^{-}, NO_3^{-}, SO_4^{2-}, K^{+}, Mg^{2+} and Ca^{2+} in atmospheric deposition samples (meq L^{-1}). The molar ratios (black dot lines) in seawater are also shown (sea-water data from Keene et al., 1986).

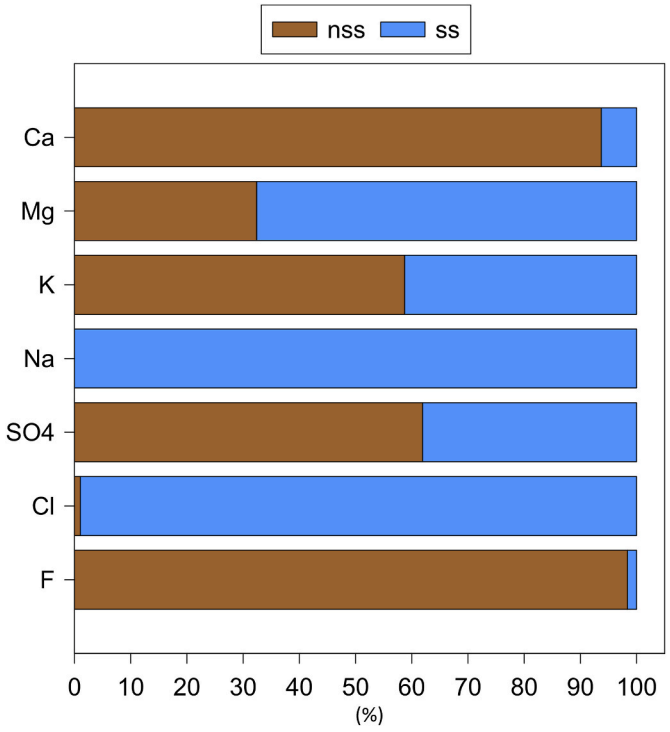

Fig. 7. Non-sea-salt (brown) and sea-salt (blue) fractions (%) for each major ion.

influence on the chemical composition of the atmospheric deposition as the distance from the coastline increases. Similar conclusions can also be drawn for Mg (median 0.066 meq L^{-1} in Palermo and 0.050 meq L^{-1} in Piana degli Albanesi). The median concentration of nss-SO_4^{2-} for the sites in the city of Palermo was similar (0.028–0.034 meq L^{-1}), higher than that measured in the Piana degli Albanesi atmospheric deposition samples, which was 0.021 meq L^{-1}. In the study area, nss-SO_4^{2-} has predominantly an anthropogenic origin, and the difference in concentrations can be explained by the greater urbanisation of the Palermo area compared to that of Piana degli Albanesi. Palermo City has shown higher median levels of nitrate concentrations (0.036 meq L^{-1}) in comparison to the Piana degli Albanesi site (0.023 meq L^{-1}). In Palermo atmospheric deposition samples, nss-SO_4^{2-} correlates with NO_3^{-} ($r = 0.71$; p-value 0.0001), suggesting a common transport mechanism rather than a reaction between their precursors (Wang et al., 2008). The most likely sources for the precursors (SO_x and NO_x) of these species were urban activities, such as household combustion and emissions from internal-combustion vehicles.

At the ARC sampling site, the highest median concentration of K^{+} was measured (0.010 meq L^{-1}), while the lowest concentration was found at Piana degli Albanesi, 0.007 meq L^{-1}. Potassium showed varying contributions from sea salt, ranging from 39.2% to 47.1%, but the primary source for this ion was different. High Ca^{2+} concentrations were observed at all monitoring sites, particularly in Palermo City, with median concentrations of 0.0148 meq L^{-1}, and 0.080 meq L^{-1} for the Piana degli Albanesi site. Calcium had a very low sea salt contribution of 6.3% and was primarily derived from the weathering of the carbonate rocks that are extensively found in the study area (Varrica et al., 2003; Montana et al., 2008). The good correlations between Ca^{2+}, nss-Mg^{2+}, nss-K^{+}, and HCO_3^{-} indicated a common terrigenous (crustal) source for these ions, as shown in Fig. 8. A minoritarian source of nss-K^{+} could be biomass burning; however, this source was certainly of little impact at the Palermo monitoring sites, whereas it may be more widespread at the Piana degli Albanesi site.

The chemical composition of Sicilian atmospheric deposition is also linked to Saharan dust minerals such as calcite, dolomite, gypsum, illite, smectite, and palygorskite (Alaimo and Ferla, 1979; Badalamenti et al., 1984; Guerzoni et al., 1999; Varrica et al., 2019). The terrigenous contribution to this chemical composition is seasonal and is carried by southerly winds from the Sahara Desert, reaching the entire Mediterranean basin and sometimes even parts of the European continent.

Anthropogenic emissions of gaseous ammonia (NH_3) and particulates containing NH_4^{+} primarily related to agricultural activities result in ammonium with no marine contributions. Homogeneous NH_4^{+} concentrations were measured in the study area at all sites, with median values over the monitoring period ranging between 0.06 meq L^{-1} for the Piana degli Albanesi site and 0.08 meq L^{-1} for the Palermo PRT site. The elements often related to anthropogenic sources (nss-SO_4^{2-}, NO_3^{-}, and NH_4^{+})

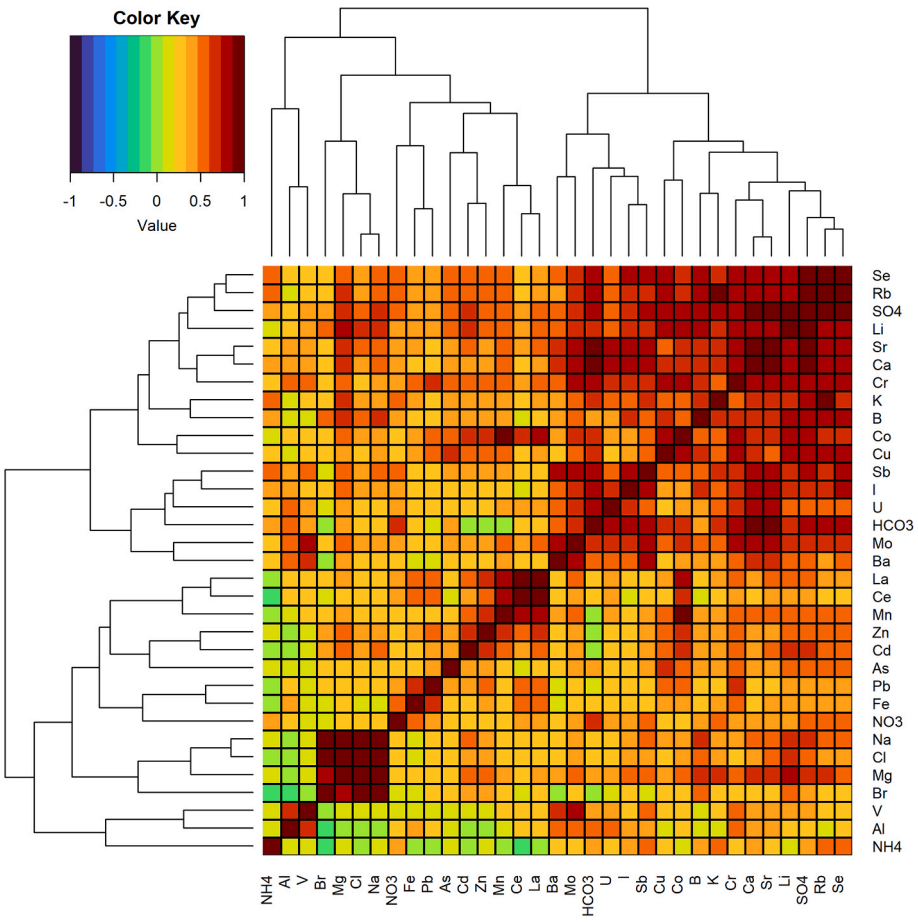

Fig. 8. Heatmaps of correlations for trace elements. Colours represent the direction of correlations from negative (blue) to positive (red), and green colour represents uncorrelated trace elements.

account for 22.2% of the total dissolved ions. Fluoride concentrations were generally low in all the monitoring sites, with the highest median value at the 4CNT sampling site (0.005 meq L^{-1}) and the lowest at Piana degli Albanesi (0.001 meq L^{-1}). Gaseous F^- compounds may derive from anthropogenic sources while the marine one is trivial (ssF^- < 2%). Fluoride had the best correlation with nss-SO_4^{2-}, r = 0.98, p-value <0.001, highlighting a possible common source.

The correlations between the major ions are useful for an initial identification of the most important sources responsible for the emission of gases and particles that influence the chemical composition of atmospheric deposition. The same approach can also be used with trace elements. The correlations between all elements, both major and trace, are shown in Fig. 8 using heatmaps. Among the major species and trace elements analysed, six of them, i.e., F-, Ti, Ni, Sn, Cs, and Tl were excluded because in many samples their concentration was < LOQ. At the top right of the heatmap, trace elements were highly positively correlated with each other; at the bottom left of the heatmap, most trace elements were uncorrelated.

5.3. Confirmatory factor analysis (CFA)

The confirmatory factor analysis model is shown in Fig. 9. The factor loadings indicate the strength and direction of the relationships. Most of the standardized factor loadings are greater than 0.50, suggesting a stronger link between the latent constructs and the observed variables. However, even if the standardized factor loading for SO_4^{2-} for the marine latent construct, Al, and Mg for the crustal latent construct and NH_4^+ and NO_3^- for anthropogenic latent construct were lower than 0.5, except for NH_4^+ in the anthropogenic latent construct they were statistically significant, indicating that they were important in the definition of the construct.

The model had a good fit both in terms of CFI = 0.953 and RMSEA = 0.072 (0.056–0.087). Overall, based on factor loadings and goodness of fit indices, the considered trace elements explained well the latent factors, i.e. anthropogenic, crustal, and marine.

5.4. Buffering and acidifying capacity of major ions

In the monitored period, the pH value of rainwater ranged from 5.2 to 9.4, with a median value of 6.5. The findings of this study were consistent with Dongarrà and Francofonte (1995) showing rainwater pH values in Palermo from 1982 to 1983 and 1988–1989, which ranged between 4.5 and 7.2. Similarly, Brugnone et al. (2023) reported median pH values of 6.3 and 6.7 in other Sicilian urban areas, Milazzo and Priolo Gargallo, respectively. The pH values were inversely related to the amount of rainfall, being the result of a relatively higher influence of the dry deposition during periods with lower precipitations. The higher quantity of solid particles present in rainwater causes larger post-deposition interactions between the water and atmospheric aerosol particles like geogenic dust and sea aerosol. These particles play a buffering role in the pH and are the main contributors to the mineralization of rainwater in Palermo (Badalamenti et al., 1984; Alaimo et al., 1989). Anthropogenic emissions are considered the primary acidifying agents of rainwater (Seinfeld and Pandis, 1998), although natural processes like volcanic emissions may also contribute locally. Thus, acid rain is generally considered evidence of anthropogenic pollution. However, in the Mediterranean area, as well as other areas with an extensive presence of geogenic dust, mainly from limestones, rainwater

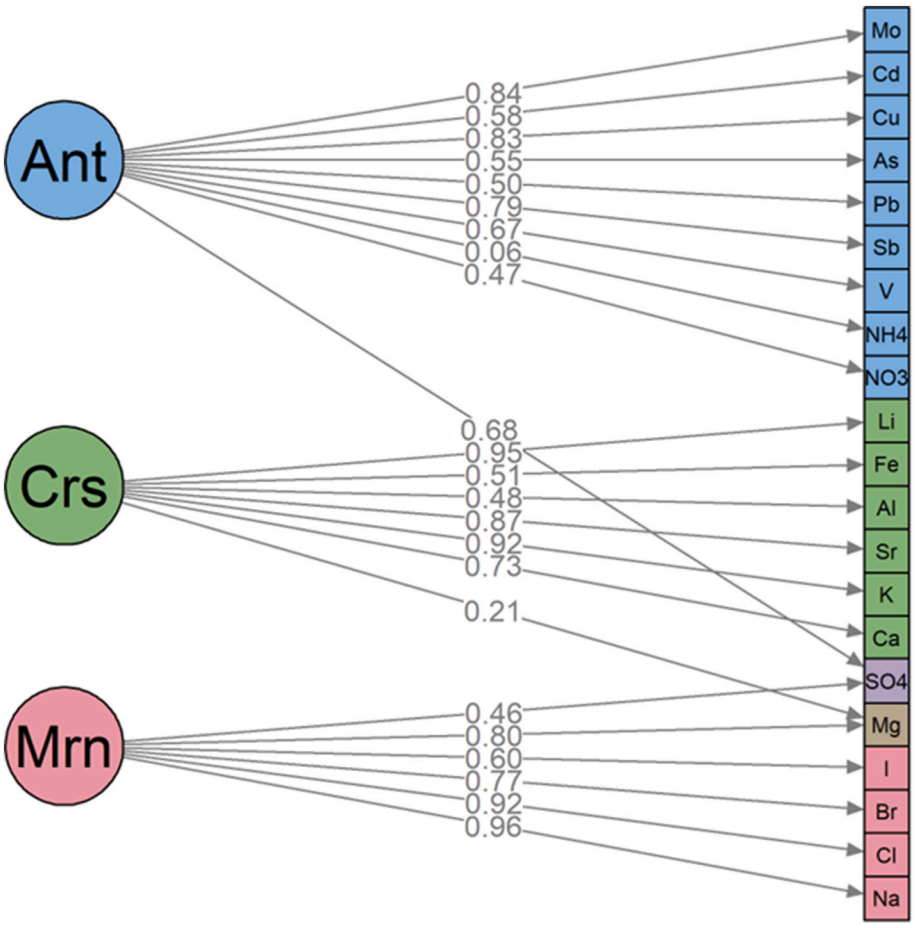

Fig. 9. Confirmatory factor analysis (CFA) model. Circles are the latent construct; squares are measured variables. Factor loadings (number in the arrow) are standardised. Ant = Anthropogenic source; Crs = crustal materials; Mrn = marine source.

is usually alkaline due to the titration of acidity by carbonate particles (Al-Momani et al., 2008; D'Alessandro et al., 2013; Brugnone et al., 2020, 2023).

Considering a value of 5.6 as the pH value expected for rainwater in equilibrium with gaseous atmospheric CO_2, most of the samples (96%) showed higher values indicating a prevailingly alkaline character for the atmospheric deposition in the study area.

In this study, nssCa^{2+} and NH_4^+ were considered the primary neutralising components of rainwater (NP), while nssSO_4^{2-} and NO_3^- acted as the primary acidifying components of rain (AP) (Huang et al., 2008). The equilibrium between acidity and alkalinity was evaluated using NP/AP, calculated as:

$$\frac{NP}{AP} = \frac{nssCa^{2+} + NH_4^+}{nssSO_4^{2-} + NO_3^-}. \quad (4)$$

The ratio varied between 1.09 and 10.2, with a median of 3.40. The highest and lowest NP/AP ratio values were recorded at the "Porto" site on April 16–30, 2015, and October 12–19, 2015, respectively. The site also had the highest median value of 4.24. At all monitoring stations, except for Piana degli Albanesi, the lowest ratio was observed during April 17–29, 2015, when there was no rainfall. The lowest value at the Piana degli Albanesi site was recorded during February 11–20, 2015 (1.19), when there was heavy rainfall (>48.7 mm), causing the collection bottle to overflow.

Interestingly, no linear correlation was observed between rainwater amount and NP/AP ratio ($r = 0.136$, p-value = 0.535). However, a weak positive linear correlation was found between pH and NP/AP ($r = 0.349$, p-value <0.001).

The high NP/AP values indicate that the natural acidity of rainwater was buffered by the atmospheric geogenic particulate matter of carbonate composition (nss-Ca^{2+}) and by NH_4^+, the latter mainly from anthropogenic sources such as agricultural practices. It is important to distinguish whether ammonia dissolves in rainwater as a gas or as solid particles of $(NH_4)_2SO_4$ or NH_4Cl since the effects are opposite in the two cases (Dongarrà and Francofonte, 1995).

The research also found that the high pH values in Palermo's rainwater were linked to the high quantity of carbonate particles in the atmosphere, which are the main CCNs of raindrops. The quantity of carbonate particles increases considerably when winds blow from the south, as they cross the inner part of Sicily before reaching Palermo. Furthermore, analysis of the particulates above Palermo revealed the presence of calcite, dolomite, quartz, and phyllosilicates (kaolinite and micas) (Alaimo and Ferla, 1979; Badalamenti et al., 1984; Alaimo et al., 1989; Alaimo et al., 1999; Calabrese et al. in prep). The incoming Saharan dust sometimes also contains talc, palygorskite, and gypsum (generally less than 2%) (Loÿe-Pilot et al., 1986). Finally, the buffering role of these ionic species was greater than the acidifying capacity of NO_3^- and nss-SO_4^{2-}, both from anthropogenic sources.

6. Conclusions

The paper investigates the chemical composition of atmospheric deposition, focusing on major ions and trace elements collected over a year from four locations in Palermo and a semi-rural site. The samples exhibited low mineralization with characteristics such as low electrical conductivity and total dissolved solids, typically showing an inverse correlation with rainfall. The pH was above 5.6, indicating buffering by

Ca^{2+} and NH_4^+. The highest concentrations of major ions were found in Palermo, linked to marine sources for Cl^-, Na^+, Mg^{2+}, and some K^+ and SO_4^{2-}. In contrast, anthropogenic sources from fossil fuel combustion contributed to nss-SO_4^{2-}, NO_3^-, and NH_4^+, while fluoride also indicated anthropogenic influence. Terrigenous sources for Ca^{2+}, HCO_3^-, nss-K^+, and nss-Mg^{2+} were traced to carbonate outcrops and Sahara dust. Trace elements showed similar sources to major ions but higher concentrations in Palermo. Elements like Ba, As, Cr, Mo, Ni, Cu, Sb, Zn, and V were mainly from vehicles and heating, while Al, Fe, Ti, and Be came from crustal materials. Confirmatory factor analysis identified three latent factors: Anthropogenic, Crustal, and Marine. The study underscores the diverse sources of ions and trace elements in atmospheric deposition, but highlights remaining questions about deposition fluxes, trace element distribution, and particulate matter composition. Further research is ongoing to address these issues.

CRediT authorship contribution statement

Filippo Brugnone: Writing – original draft, Methodology, Investigation, Formal analysis, Data curation, Conceptualization. **Walter D'Alessandro:** Writing – review & editing, Methodology, Investigation, Conceptualization. **Marcello Liotta:** Writing – review & editing, Methodology, Investigation, Data curation, Conceptualization. **Marcello Bitetto:** Writing – review & editing, Investigation. **Luciana Randazzo:** Writing – review & editing, Methodology, Investigation, Conceptualization. **Sergio Bellomo:** Investigation. **Lorenzo Brusca:** Writing – review & editing, Investigation, Formal analysis. **Giovanna Cilluffo:** Writing – review & editing, Formal analysis, Data curation. **Francesco Parello:** Conceptualization. **Sergio Calabrese:** Writing – original draft, Methodology, Investigation, Formal analysis, Data curation, Conceptualization.

Funding

We would like to thank the University of Palermo, which adhered to the transformation contract signed between CRUI-CARE and Elsevier (Science Direct), and allowed us to publish in open access format without charge.

Declaration of competing interest

The authors declare that they have no known competing financial interests or personal relationships that could have appeared to influence the work reported in this paper.

Acknowledgments

The authors wish to thank all the people who have logistically supported our sampling and the bibliographic research, including Cosimo Rubino. We thank SIAS - Servizio Informativo Agrometeorologico Siciliano for the meteorological data.

Appendix A. Supplementary data

Supplementary data to this article can be found online at https://doi.org/10.1016/j.apr.2025.102431.

References

Alaimo, R., Ferla, P., 1979. Presenza di palygorskite nella polvere trasportata dallo "scirocco". In: Sicilia: Implicazioni Geologiche Ed Ambientali, vol. 4. Ist. Min. Petrol. Geochim., Palermo, Quaderno n.

Alaimo, R., Deganello, S., Di Franco, L., Montana, G., 1989. Caratteristiche composizionali del particolato solido atmosferico chimismo delle acque di precipitazione nell'area urbana di Palermo. In: Proceedings of the International Symposium. The Conservation of Monuments in the Mediterranean Basin, Bari.

Alaimo, M.G., Dongarrà, G., Melati, M.R., Monna, F., Varrica, D., 1999. Recognition of environmental trace metal contamination using pine needles as bioindicators. The urban area of Palermo (Italy). Environ. Geol. 39, 914–923.

Alastuey, A., Querol, X., Chaves, A., Ruiz, C.R., Carratala, A., Lopez-Soler, A., 1999. Atmospheric deposition in a rural area located around a large coal fired power station, northeast Spain. Environ. Pollut. 106, 359–367. https://doi.org/10.1016/s0269-7491(99)00103-7.

Al-Momani, I.F., Momani, K.A., Jaradat, Q.M., Massadeh, A.M., Yousef, Y.A., Alomary, A. A., 2008. Atmospheric deposition of major and trace elements in Amman, Jordan. Environ. Monit. Assess. 136, 209–218. https://doi.org/10.1007/s10661-007-9676-4.

APHA, AWWA, WEF, 2005. Standard Methods for the Examination of Water and Wastewater, twenty-first ed. American Public Health Association, Washington D.C., U.S.A.

Arsene, C., Olariu, R.I., Mihalopoulos, N., 2007. Chemical composition of rainwater in the northeastern Romania, Iasi region (2003-2006). Atmos. Environ. 41 (40), 9452–9467. https://doi.org/10.1016/j.atmosenv.2007.08.046.

Badalamenti, F., Carapezza, M., Dongarrà, G., Macaluso, A., Hauser, S., Parello, F., 1984. Precipitazioni atmosferiche in Sicilia. 1) L'area urbana di Palermo. Rend. Soc. It. Mineral. e Petrol. 39 (1), 81–92.

Bentler, P.M., 1990. Comparative fit indexes in structural models. Psychol. Bull. 107 (2), 238–246. https://doi.org/10.1037/0033-2909.107.2.238.

Bolle, H.J., 2003. Climate, climate variability, and impacts in the mediterranean area: an overview. In: *Mediterranean Climate*. Regional Climate Studies. Springer, Berlin, Heidelberg. https://doi.org/10.1007/978-3-642-55657-9_2.

Bonardi, G., De Capoa, P., Staso, A. Di, Estévez, A., Martín-Martín, M., Martín-Rojas, I., Perrone, V., Tent-Manclús, J.E., 2003. Oligocene-to-early miocene depositional and structural evolution of the Calabria-Peloritani Arc southern terrane (Italy) and geodynamic correlations with the Spain betics and Morocco rif. Geodin. Acta 16 (2–6), 149–169. https://doi.org/10.1016/j.geoact.2003.06.001.

Brocard, D., Lacaux, J.P., Eva, H., 1998. Domestic biomass combustion and associated atmospheric emissions in West Africa. Global Biogeochem. Cycles 12 (1), 127–139. https://doi.org/10.1029/97GB02269.

Brugnone, F., D'Alessandro, W., Calabrese, S., Li Vigni, L., Bellomo, S., Brusca, L., Prano, V., Saiano, F., Parello, F., 2020. A Christmas gift: signature of the 24th December 2018 eruption of Mt. Etna on the chemical composition of atmospheric deposition in eastern Sicily. Italian Journal of Geosciences 139 (3), 1–18. https://doi.org/10.3301/ijg.2020.08.

Brugnone, F., D'Alessandro, W., Parello, F., Liotta, M., Bellomo, S., Prano, V., Li Vigni, L., Sprovieri, M., Calabrese, S., 2023. Atmospheric deposition around the industrial areas of Milazzo and Priolo Gargallo (sicily, Italy) - Part A: major ions. Int. J. Environ. Res. Publ. Health 20, 3898. https://doi.org/10.3390/ijerph20053898.

Calabrese, S., Aiuppa, A., Allard, P., Bagnato, E., Bellomo, S., Brusca, L., Parello, F., 2011. Atmospheric sources and sinks of volcanogenic elements in a basaltic volcano (Etna, Italy). Geochem. Cosmochim. Acta 75 (23), 7401–7425. https://doi.org/10.1016/j.gca.2011.09.040.

Catalano, R., Agate, M., Albanese, C., Avellone, G., Basilone, L., Gasparo Morticelli, M., Gugliotta, C., Sulli, A., Valenti, V., Gibilaro, C., Pierini, S., 2013. Walking along a crustal profile across the sicily Fold and Thrust Belt. In: AAPG International Conference & Exhibition, 23-26 October 2011, Milan, Italy, Post-Conference Field Trip 4/27-29 October 2011. Geol. F. Trips, pp. 61–78. https://doi.org/10.3301/GFT.2013.05, 5, no. 2.3.

Cheng, M.C., You, C.F., 2010. Sources of major ions and heavy metals in rainwater associated with typhoon events in southwestern Taiwan. J. Geochem. Explor. 105, 106–116.

Chesselet, R., Morelli, M., Buat-Menard, P., 1972. Some aspects of the geochemistry of marine aerosols. In: Dyrssen, D., Jagner, D. (Eds.), The Changing Chemistry of the Oceans, Proceedings of Nobel Symposium 20. Wiley-Interscience, New York, p. 92.

Conradie, E.H., Van Zyl, P.G., Pienaar, J.J., Beukes, J.P., Galy-Lacaux, C., Venter, A.D., Mkhatshwa, G.V., 2016. The chemical composition and fluxes of atmospheric wet deposition at four sites in South Africa. Atmos. Environ. 146, 113–131. https://doi.org/10.1016/j.atmosenv.2016.07.033.

D'Alessandro, W., Katsanou, K., Lambrakis, N., Bellomo, S., Brusca, L., Liotta, M., 2013. Chemical and isotopic characterisation of bulk deposition in the Louros basin (Epirus, Greece). Atmos. Res. 132–133, 399–410. https://doi.org/10.1016/j.atmosres.2013.07.007.

Doglioni, C., Merlini, S., Cantarella, G., 1999. Foredeep geometries at the front of the apennines in the ionian sea (central mediterranean). Earth Planet Sci. Lett. 168, 243–254.

Dongarrà, G., Francofonte, S., 1995. The quality of rainwaters: a geochemical process of water-air-rock-life interaction. Environ. Geol. 25, 149–155.

Gaertner, M.A., Jacob, D., Gil, V., Domínguez, M., Padorno, E., Sánchez, E., Castro, M., 2007. Tropical cyclones over the Mediterranean Sea in climate change simulations. Geophys. Res. Lett. 34 (14), L14711. https://doi.org/10.1029/2007GL029977.

Galy-Lacaux, C., Laouali, D., Descroix, L., Gobron, N., Liousse, C., 2009. Long term precipitation chemical composition and wet deposition in a remote dry savanna site in Africa (Niger). Atmos. Chem. composition and Phys. 9 (5), 1579–1595. https://doi.org/10.5194/acp-9-1579-2009.

Guerzoni, S., Molinaroli, E., Rossini, P., Rampazzo, G., Quarantotto, G., De Falco, G., Cristini, S., 1999. Role of desert aerosol in metal fluxes in the Mediterranean area. Chemosphere 39, 229–246. https://doi.org/10.1016/S0045-6535(99)00105-8.

Houze Jr., R.A., 1993. Cloud Dynamics. Academic Press, p. 573.

Huang, Y.L., Wang, Y.L., Zhang, L.P., 2008. Long-term trend of the chemical composition of wet atmospheric precipitation during 1986-2006 at Shenzhen City, China. Atmos. Environ. 42 (16), 3740–3750. https://doi.org/10.1016/j.atmosenv.2007.12.063.

EMEP/CCC, 2009. Manual for sampling and chemical analysis. EMEP Cooperative Program for Monitoring and Heavy Metals and POP Measurements 2009, NILU: EMEP/CCC.

Istituto Nazionale di Statistica (ISTAT).http://dati.istat.it/Index.aspx?DataSetCode=DCIS_POPRES1#(accessed 26 February 2023).

Kajino, M., Aikawa, M., 2015. A model validation study of the washout/rainout contribution of sulfate and nitrate in wet deposition compared with precipitation chemical composition data in Japan. Atmos. Environ. 117, 124–134. https://doi.org/10.1016/j.atmosenv.2015.06.042.

Keene, W.C., Pszenny, A.A.P., Galloway, J.N., Hawley, M.E., 1986. Sea-salt corrections and interpretation of constituent ratios in marine precipitation. J. Geophys. Res. 91 (D6), 6647. https://doi.org/10.1029/jd091id06p06647.

Kitto, M.E., 1993. Trace element patterns in fuel oils and gasoline for use in source apportionment. J. Air Waste Manag. Assoc. 43, 1381–1388.

Lelieveld, J., 1993. Multiphase processes in the atmospheric sulfur cycle. In: Wollast, R. (Ed.), Interactions of C, N, P and S Biogeochemical Cycles and Global Change, pp. 305–331.

Lionello, P.J., Bhend, J., Buzzi, A., Della-Marta, P.M., Krichak, S.O., Jansa`, A., Maheras, P., Sanna, A., Trigo, I.F., Trigo, R., 2006. Cyclones in the Mediterranean region: climatology and effects on the environment. Developments in Earth and Environmental Sciences 4, 325–372. https://doi.org/10.1016/S1571-9197(06)80009-1.

Liotta, M., Shamavu, P., Scaglione, S., D'Alessandro, W., Bobrowski, N., Bruno Giuffrida, G., Calabrese, S., 2017. Mobility of plume-derived volcanogenic elements in meteoric water at Nyiragongo volcano (Congo) inferred from the chemical composition of single rainwater events. Geochem. Cosmochim. Acta 217, 254–272. https://doi.org/10.1016/j.gca.2017.08.001.

Loÿe-Pilot, M.D., Martin, J.M., Morelli, J., 1986. Influence of Saharan dust on the rain acidity and atmospheric input to the Mediterranean. Nature 321, 427–428. https://doi.org/10.1038/321427a0.

Mariotti, A., Struglia, M.V., Zeng, N., Lau, K.M., 2002. The hydrological cycle in the Mediterranean region and implications for the water budget of the Mediterranean sea. J. Clim. 15 (13), 1674–1690. https://doi.org/10.1175/15200442(2002)015<1674:THCITM>2.0.CO;2.

Menichini, E., 2006. Metodi per la determinazione di arsenico, cadmio, nichel e idrocarburi policiclici aromatici nelle deposizioni atmosferiche. Italianist: Ist. Superiore di Sanità 2006 23. Rapporti ISTISAN 06/38 (accessed 06 April 2023).

Montana, G., Randazzo, L., Oddo, I.A., Valenza, M., 2008. The growth of "black crusts'' on calcareous building stones in Palermo (Sicily): a first appraisal of anthropogenic and natural sulphur sources. Environ. Geol. 56 (2), 367–380. https://doi.org/10.1007/s00254-007-1175-y.

NASA - MERRA 2. https://gmao.gsfc.nasa.gov/reanalysis/MERRA-2/(accessed 26 February 2023).

Ondov, J.M., Zoller, W.H., Gordon, G.E., 1982. Trace element emissions on aerosols from motor vehicles. Environ. Sci. Technol. 16, 318–328.

Prasad Shukla, S., Mukesh, S., 2010. Neutralization of rainwater acidity at Kanpur, India. Tellus Ser. B 62 (3), 172–180. https://doi.org/10.1111/j.1600-0889.2010.00454.x.

Safai, P.D., Rao, P.S.P., Momin, G.A., Ali, K., Chate, D.M., Praveen, P.S., 2004. Chemical composition of precipitation during 1984–2002 at Pune, India. Atmos. Environ. 38 (12), 1705–1714. https://doi.org/10.1016/j.atmosenv.2003.12.016.

Santos, P.S.M., Otero, M., Santos, E.B.H., Duarte, A.C., 2011. Chemical composition of rainwater at a coastal town on the southwest of Europe: what changes in 20 years? Sci. Total Environ. 409, 3548–3553.

Schlesinger, W.H., Hartley, A.E., 1992. A global budget for atmospheric NH_3. Biogeochemistry 15, 191–211. https://doi.org/10.1007/BF00002936.

Schmidt, F., Hinrichs, K.U., Elvert, M., 2010. Sources, transport, and partitioning of organic matter at a highly dynamic continental margin. Marine Chemical composition 118 (1–2), 37–55. https://doi.org/10.1016/j.marchem.2009.10.003.

Seinfeld, J.H., Pandis, S.N., 1998. Atmospheric Chemical Composition and Physics from Air Pollution to Climate Change. John Wiley and Sons, New York. Incorporated.

Steiger, J.H., 2010. Structural model evaluation and modification: an interval estimation approach. Multivariate Behav. Res. 25 (2), 173–180. https://doi.org/10.1207/s15327906mbr2502_4.

Tang, A., Zhuang, G., Wang, Y., Yuan, H., Sun, Y., 2005. The chemical composition of precipitation and its relation to aerosol in Beijing. Atmos. Environ. 39 (19), 3397–3406. https://doi.org/10.1016/j.atmosenv.2005.02.001.

Thurston, G.D., Spengler, J.D., 1985. A quantitative assessment of source contributions to inhalable particulate matter pollution in metropolitan Boston. Atmos. Environ. 19 (1), 9–25. https://doi.org/10.1016/0004-6981(85)90132-5.

Varrica, D., Dongarrà, G., Sabatino, G., Monna, F., 2003. Inorganic geochemistry of roadway dust from the metropolitan area of Palermo (Italy). Environ. Geol. 44, 222–230. https://doi.org/10.1007/s00254-002-0748-z.

Varrica, D., Tamburo, E., Vultaggio, M., Di Carlo, I., 2019. ATR–FTIR Spectral analysis and soluble components of PM10 and PM2.5 particulate matter over the urban area of Palermo (Italy) during normal days and saharan events. Int. J. Environ. Res. Publ. Health 16, 2507. https://doi.org/10.3390/ijerph16142507.

Wang, L., Soda, M., Ueda, T., 2008. Simulation of Chloride Diffusivity for Cracked Concrete Based on RBSM and Truss Network Model. J. Adv. Concr. Technol. 6 (1), 143–155. https://doi.org/10.3151/jact.6.143.

WMO – World Meteorological Organization, 2018. Guide to Meteorological Instrument and Observing Practice. Geneva.

WMO – World Meteorological Organization – Global Atmosphere Watch Programme (GAW). https://public.wmo.int/en/programmes/global-atmosphere-watch-programme (accessed 26 February 2023).